PHYSICAL REVIEW B **81**, 064102 (2010)

Identification of vacancy defects in a thin film perovskite oxide

D. J. Keeble,[1,*] R. A. Mackie,[1] W. Egger,[2] B. Löwe,[2] P. Pikart,[3] C. Hugenschmidt,[3] and T. J. Jackson[4]
[1]*Carnegie Laboratory of Physics, School of Engineering, Physics, and Mathematics, University of Dundee, Dundee DD1 4HN, United Kingdom*
[2]*Universität Bundeswehr München, D-85577 Neubiberg, Germany*
[3]*Technische Universität München, ZWEFRM 11 E21, D-85747 Garching, Germany*
[4]*Department of Electronic, Electrical and Computer Engineering, University of Birmingham, Birmingham B15 2TT, United Kingdom*
(Received 13 January 2010; published 2 February 2010)

Vacancies are the dominant point defects in perovskite oxides, however, detecting and identifying the nature of vacancy defects in thin films remains challenging. This can be achieved using electron-beam methods but concentrations of several percent are required. Here we use a high-flux positron beam, providing high statistics positron lifetime measurements, to identify vacancies in laser ablated $SrTiO_3$ on $SrTiO_3$. The method is capable of subparts per million sensitivity and when combined with density-functional theory provides local structure information. The positron lifetime spectrum depth profile detects the presence of large vacancy clusters in a surface layer, a uniform distribution of Sr vacancies through the bulk of the film and resolves the interface with the substrate.

DOI: 10.1103/PhysRevB.81.064102 PACS number(s): 68.55.Ln, 77.84.Ek, 78.70.Bj

I. INTRODUCTION

The ability to produce high-quality perovskite oxide, ABO_3, thin films and heterostructures has led the development of oxide electronics,[1–4] and to an increase in our understanding of ferroic and multiferroic materials.[5,6] The marked improvements in the structural quality of perovskite oxide layers will ultimately result in the electronic properties being limited by the presence of electrically active point defects at subparts per million concentration levels. Ferroic perovskite oxides are typically wide band-gap semiconductors with $E_g \sim 3.5-4.1$ eV.[1] Point defects in ferroics can alter material properties in two ways; they act, as in conventional semiconductors, as charge sources, sinks, and recombination centers, but in addition the strain and electric fields associated with the defect can interact directly with the mesoscopic polarization and, for example, pin domain walls.[7]

Knowledge on the point defect content of bulk perovskite oxide materials has traditionally been obtained from measurements of high-temperature electrical conductivity as a function of oxygen partial pressure, interpreted using defect chemistry,[8] and supplemented, for example, by Hall, Seebeck, or more recently optical and impedance spectroscopy measurements.[9] Local probe spectroscopy methods give complementary insight, they can provide local structure information allowing atomic scale characterization of specific point defects. For example, vacancy defect complexes with a net local dipole moment are of particular relevance. Electron magnetic-resonance methods have the required sensitivity and can provided detailed local structure models for those centers with a paramagnetic ground state.[10] However, convincing evidence is lacking that the isolated native vacancy defects have accessible EPR active states in perovskite oxides.[11] Direct imaging of O vacancies has been demonstrated using aberration corrected transmission electron microscopy (TEM) (Ref. 12) or annular-dark-field TEM, supported by electron energy-loss spectroscopy.[13] Electron energy-loss near-edge structures combined with first-principles calculations provided evidence for high concentrations of Sr vacancies in the vicinity of grain boundaries, resulting from heat treatments.[14] However, these methods typically require defect concentrations greater than 1% and are time consuming and destructive.

Here we report the detection of a Sr vacancy-related defect distribution in a thin film of the perovskite oxide $SrTiO_3$ grown by laser ablation using positron lifetime measurements performed with a high intensity variable energy positron beam. The dominant positron lifetime component in the thin film at ~260 ps is due to trapping at Sr vacancy-related defects. Vacancy cluster defects with a lifetime of ~410 ps were also detected. A near surface, ~50 nm, layer was resolved and showed an increase in trapping to large vacancy clusters or nanovoids. Previous positron-annihilation studies of oxide thin films have typically been performed using conventional positron beams with two to three orders of magnitude lower intensity and have used Doppler broadening spectroscopy (DBS) which gives less direct information on the nature of the trapping vacancy.

An implanted positron will thermalize within a few picoseconds then annihilate in the material from a state i with a lifetime τ_i and a probability I_i. This can be a delocalized state in the bulk lattice, or a localized state at a vacancy defect, or if the open-volume defect has sufficient size (e.g., in nanovoids) the electron-positron bound state known as positronium can be formed. If the average positron lifetime, $\bar{\tau} = \Sigma_i I_i \tau_i$, is greater than the bulk, i.e., perfect lattice, positron lifetime, τ_B (a characteristic of the material), this indicates that vacancy-type defects are present. The rate of positron trapping to a vacancy, κ_d, is proportional to the concentration of these defects, $[d]$, where the constant of proportionality is the defect specific trapping coefficient, μ_d; $\kappa_d = \mu_d[d]$. While vacancy defects, due to the lack of a positive-ion core, form

TABLE I. Positron lifetime values (ps) calculated by the DFT method MIKA for monovacancy and vacancy nearest-neighbor complexes in $SrTiO_3$ (relaxed structure calculations in parentheses). LMTO DFT method values from Ref. 19 are also shown.

	Bulk	V_O	$V_{O\text{-}O}$	V_{Ti}	$V_{Ti\text{-}O}$	V_{Sr}	$V_{Sr\text{-}O}$	$V_{Sr\text{-}3O}$	$V_{Sr\text{-}Sr}$	$V_{Ti\text{-}O\text{-}Ti}$	$V_{Ti\text{-}3O\text{-}Sr}$
MIKA-AP	151	166 (170)	178	195 (184)	225	279 (279)	283	289	283	247	316
LMTO-AP	146	159		194		252					

an attractive potential the local charge must also be considered, if positive a Coulomb barrier inhibits trapping, however, for neutral or negative defects trapping coefficients are large, typically in the range 0.5×10^{15}–6×10^{15} s^{-1} at., giving the method subparts per million concentration sensitivity.[15]

The one defect simple trapping model predicts two experimental positron lifetimes; $\tau_2=\tau_d$ is the lifetime characteristic of the defect and the first lifetime, τ_1, is reduced from the bulk, or perfect lattice, lifetime, τ_B, by an amount that depends on the rate of trapping to the defect, so that $\tau_1 \leq \tau_B$. The model is readily extended to two or more defects and allows defect positron trapping rates, κ_d, to be determined.[15] As the concentration of vacancies increases, the intensity of the longer defect lifetime, I_2, increases toward unity. Eventually saturation trapping occurs where all positrons annihilate from the defect and sensitivity to concentration is restricted or lost completely; assuming a specific trapping coefficient $\sim2\times10^{15}$ s^{-1} at. and $\tau_B=150$ ps this would occur for a concentration of the order of 50 ppm ($\kappa_d\tau_B=\mu_d[d]\tau_B\approx10$).

The positron lifetimes for perfect material and for specific types of vacancy defect can be calculated using density-functional theory (DFT) methods. The dominant approach involves the superposition of free atomic electron densities and has been applied to positron lifetime calculations in perovskite titanate oxides.[16–19] More recently the self-consistent linear muffin-tin orbital (LMTO) method has also been applied and was found to give similar results.[19] The positron lifetime values for $SrTiO_3$ obtained by DFT methods are given in Table I.[19] The lifetimes for positrons trapped at localized states in cation vacancies are significantly larger than the ~150 ps obtained for the perfect lattice, bulk, state. Experimental lifetimes of ~181 ps for the Ti vacancy and ~275 ps for Sr vacancy-related defects have been inferred from studies of single crystal $SrTiO_3$, and along with the bulk lifetime, are consistent with the DFT values.[19]

Variable energy positron-annihilation spectroscopy (VE-PAS) methods have been applied to the study of thin film perovskite oxide materials and have demonstrated the presence of open-volume defects.[20–25] However, these studies have been largely performed using DBS were the line shape of the 511 keV annihilation radiation energy spectrum is measured. The spectrum is broadened due to the finite momentum of the electron with which the positron annihilates. Analysis of VE-DBS is normally performed using a line shape parameter, the *S* parameter. The *S* value is a measure of the fraction of positrons annihilating with low momentum, mainly valence, electrons and is typical defined as the fraction events occurring in the range $|p_L|<\sim3\times10^{-3}m_0c$, where p_L is the longitudinal component of the positron-electron pair momentum. Positron trapping to vacancy-related defects results in an increase in *S* parameter compared to perfect material. The magnitude of the increase can provide insight on the type and size of the open-volume defect trapping positrons, and on defect density. An increase in positron trapping to vacancy defects has been observed due to thin film processing in an oxygen deficient environment,[20–23] or to the formation of charge compensating vacancy defects resulting from donor impurity ion doping,[26] or due to the film growth conditions.[25] By contrast, positron lifetime values are characteristic of specific defect types and multiple positron states can be directly resolved. A single variable energy positron-annihilation lifetime spectroscopy (VE-PALS) measurement has been reported on a sample of molecular-beam epitaxy (MBE) grown thin film of $BaTiO_3$ deposited on a $SrTiO_3$ substrate.[24] The implantation energy (10 keV) was chosen to sample the substrate immediately behind the film and reported a dominant lifetime value of 165(1) ps attributed to oxygen vacancy defects generated in the near-interface region of the substrate by the MBE film growth process.

II. EXPERIMENT

Measurements were performed on a thin film of $SrTiO_3$ deposited by pulsed laser ablation on $SrTiO_3$.[27] The thickness was determined to be 603(6) nm by TEM. A KrF excimer laser was used, giving a fluence at the target surface of 1.5 J cm^{-2}. The film was grown using 5000 pulses at a repetition rate of 0.15 Hz, with a temperature 750 °C and the oxygen partial pressure was 40 Pa. Double side polished (100) single crystal $SrTiO_3$, supplied by MaTecK GmbH, was also studied. Positron-annihilation measurements were performed at the high intensity neutron-induced positron source at the Munich research reactor FRMII with a primary moderated beam intensity of $5\times10^8e^+$ s^{-1} at an energy of 1 keV.[28] Variable energy positron-annihilation lifetime spectroscopy measurements were made with the pulsed beam instrument comprising a prebuncher, chopper, and main buncher operating at 50 MHz providing the time structure and start timing signal, the annihilation radiation from the implanted positrons was detected using BaF_2 scintillation detector.[29] The beam energy could be varied between 0.5 and 22 keV. The lifetime spectra contained an average of 5.8×10^6 counts accumulated with a count rate of ~6×10^3 s^{-1}, the instrument timing resolution function was normally described by three dominant, energy dependent, terms; these showed a mean width, averaged over all energies, of 306 ps. In addition, measurements were made with the beam transported to the DBS instrument.[30]

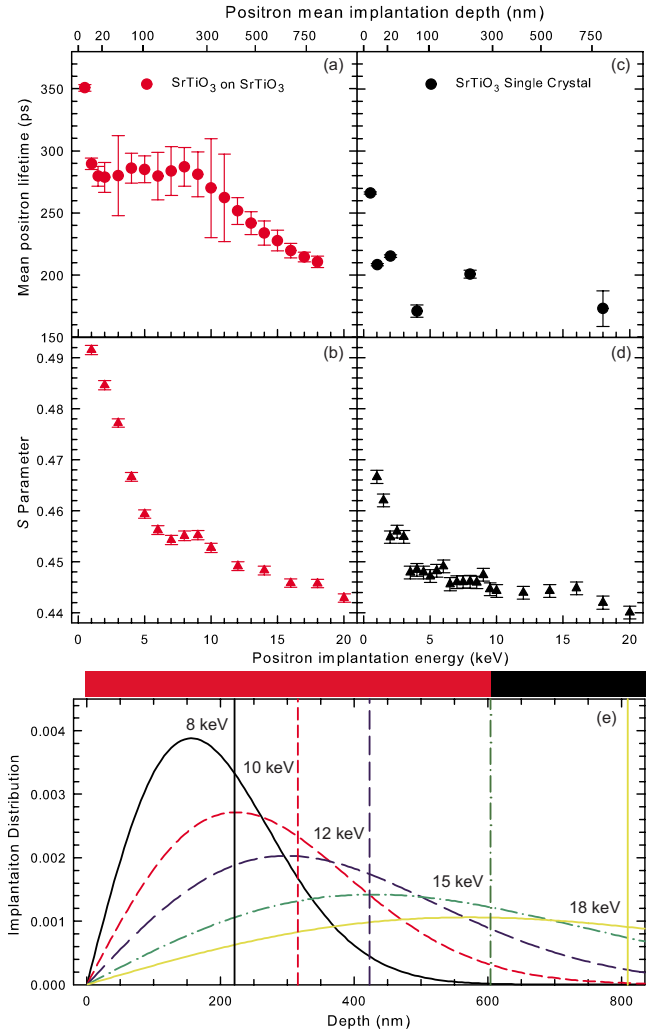

FIG. 1. (Color online) Mean positron lifetimes against positron implantation energy, measured by variable energy positron beam positron-annihilation lifetime spectroscopy, for (a) $SrTiO_3$ thin film on $SrTiO_3$ and (c) $SrTiO_3$ single-crystal substrate. The Doppler broadening spectroscopy detected low-momentum fraction S parameter depth profiles for the two samples are shown in (b) and (d), respectively. The Makhovian positron implantation profiles calculated for $SrTiO_3$ are shown in (e).

III. RESULTS AND DISCUSSION

The mean positron lifetime as a function of positron implantation energy for the laser ablated $SrTiO_3$ on $SrTiO_3$ sample is shown in Fig. 1(a). This decreases rapidly from ~350 ps at the surface to ~280 ps, and remains at this value through the bulk of the film. The onset of a reduction from ~280 ps occurs at ~9 keV, from which point the broadened Makhovian implantation profiles increasingly penetrate beyond the film-substrate interface at ~600 nm and sample the substrate, as shown in Fig. 1(e). From the large value of the mean lifetime, $\bar{\tau}$, ~280 ps in the film, knowing τ_B, and considering a plausible range of defect specific trapping coefficients, it can be concluded that the positrons are saturation trapped at vacancy defects.

Figure 1(c) shows measurements on the single-crystal $SrTiO_3$ substrate, the mean lifetime, $\bar{\tau}$, decreasing rapidly

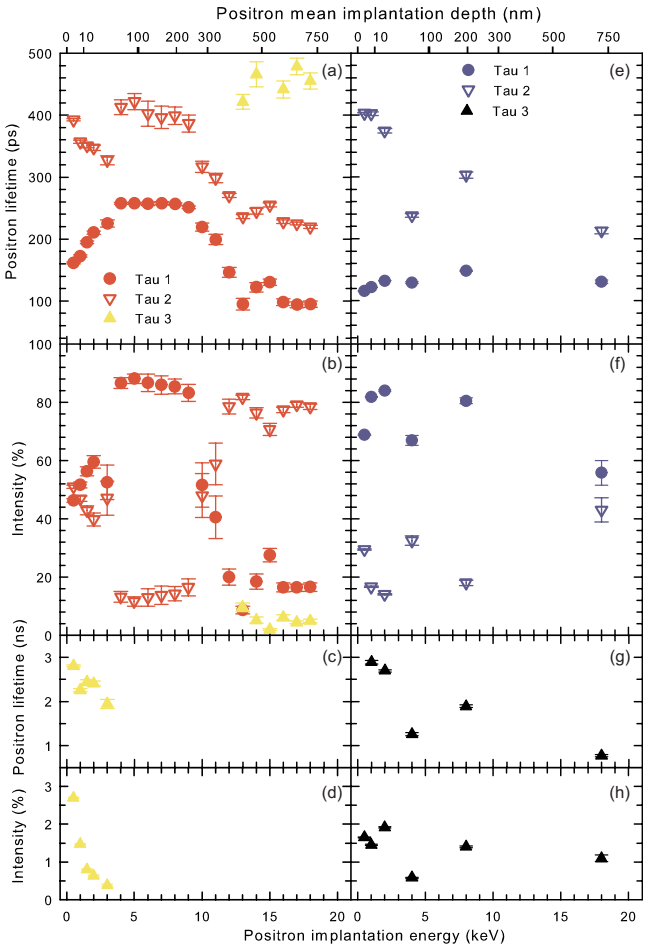

FIG. 2. (Color online) The results of multiexponential positron lifetime deconvolution for [(a)–(d)] $SrTiO_3$ thin film on $SrTiO_3$ and [(e)–(h)] $SrTiO_3$ single-crystal substrate.

from a near-surface value of 266 to ~170 ps. The $\bar{\tau}$ obtained by conventional PALS,[19] using unmoderated positrons implanting to a continuous distribution of depths down to ~0.2 mm, was 167 ps.

The rapidly accumulated high number of counts, the well-defined instrument timing resolution, and the lack of positron source annihilation terms, allowed reliable multiexponential deconvolution of the spectra. The results for the $SrTiO_3$ on $SrTiO_3$ thin film and the $SrTiO_3$ single crystal are shown in Fig. 2. The average fit chi-squared values were 1.15(9) and 1.16(10), respectively, and three lifetime components were resolved. The variation in lifetime values and intensities with implantation depth for the laser ablated film clearly show a ~50 nm surface region below which the vacancy defect densities remain constant through the film, the interface with the substrate is then clearly observed. Positrons implanted with energies greater than ~9 keV increasingly sample the film interface and substrate. At the highest implantation energies the dominant lifetime values are tending to those observed below the near-surface region of the single-crystal sample.

The top layer of the $SrTiO_3$ film is characterized by observation of long third lifetime component with a value decreasing from ~3 to 2 ns from the surface with a concomi-

tant decrease in intensity, Figs. 2(c) and 2(d). This is consistent with pick-off annihilation events due to the formation of orthopositronium in large vacancy clusters or nanovoids and with a possible contribution from back diffusion to the surface followed by positronium formation.[15] The intensity of the ~320–400 ps component in the near-surface layer [Figs. 2(a) and 2(b)] indicates the presence of larger vacancy cluster defects.

The uniform values for the lifetime and intensities of the resolved components the $SrTiO_3$ film were observed below this surface layer for implantation energies between 4 and 8 keV; the two main components were $\tau_1=257(1)$ ps, $I_1=87(1)\%$ and $\tau_2=407(10)$ ps, $I_2=13(1)\%$. A third nanosecond component had an intensity of 0.26(3)% through this energy range and has been omitted from Figs. 2(a)–2(d) for clarity.

The dominant lifetime component, ~257 ps (~87%), in the main extent of the thin film has a value slightly less than that determined for V_{Sr}, ~275 ps. A similar ~260 ps lifetime was observed for electron irradiated $SrTiO_3$ and vacuum annealed $SrTiO_3$ where the pretreatment samples showed a component attributable to Ti vacancies.[19] Saturation trapping to both Ti (~181 ps) and Sr (~275 ps) vacancies result, due to the finite instrument resolution function, in a single intermediate value lifetime component, a weighted average determined by the ratio of the vacancy concentrations and the defect specific trapping coefficients for the two defects ($\mu_{V_{Ti}}[V_{Ti}]/\mu_{V_{Sr}}[V_{Sr}]$). The defect specific trapping rate for the *B*-site vacancy is greater than that for *A* site,[18] assuming they differ by a factor 2 then simulations, similar to those described in Ref. 19, show $[V_{Sr}]>4[V_{Ti}]$ would be required to obtain a component lifetime close to 260 ps.[19] The differences in the lifetimes between isolated Sr monovancancies, and V_{Sr}-nV_O complexes, see Table I, are small and cannot be reliably differentiated.

The low intensity second lifetime component, 407(10) ps, observed for the same implantation energies [Figs. 2(a) and 2(b)] is due to open-volume defects larger than monovacancy or cation vacancy nearest-neighbor oxygen vacancy complexes (Table I). Here the MIKA-DFT calculations have been extended, using 1080 atom supercells, to cation divacancy complexes, see Table I. Comparable lifetime values were obtained for Sr divacancy defects with or without oxygen vacancy nearest neighbors of ~283 ps, similarly linear configuration Ti divacancy defects with between one and three oxygen vacancy nearest neighbors gave lifetime values between 247 and 253 ps, respectively. The largest value, 316 ps, was obtained for a Ti-Sr divacancy with three nearest-neighbor oxygen vacancies. These calculations provide evidence that the experimental lifetime corresponds to a larger vacancy cluster defect.

The component positron lifetimes for the $SrTiO_3$ single-crystal substrate are shown in Figs. 2(e)–2(h). Three lifetime components are required to fit the data reliably; a low intensity, 1.4(5)%, 1–2 ns orthopositronium pick-off third lifetime, a dominant short lifetime varying from ~115 ps at 0.5 keV near the surface to ~140 ps at 18 keV (corresponding to a mean implantation depth of ~750 nm) and a second lifetime varying from 403 to 213 ps, with increasing intensity, over the same implantation range. The PALS spectra obtained using unmoderated positrons from the sample were fitted using two lifetime components with a chi-squared of 1.009 and gave $\tau_1=123(3)$ ps, $I_1=45(4)\%$, and $\tau_2=202(3)$ ps, with appropriate resolution function and source correction terms included.

These results provide evidence that the polished crystal contains larger open-volume defects giving rise to both the nanosecond component and the ~400 ps component, and that these are mainly confined to the top few hundred nanometers. However, in contrast to the thin film, a short reduced bulk positron lifetime component is clearly resolved and is due to a fraction of annihilation events coming from perfect lattice. The lifetimes detected at 18 keV, and using conventional PALS, are in agreement with previous studies on as-received $SrTiO_3$ crystal samples,[19] the ~200 ps component can be attributed to unresolved contributions from V_{Ti} and V_{Sr} defects with concentrations in the ~0.1–1 ppm range.

Further insight can be obtained on the interface of the $SrTiO_3$ thin film with the substrate. The variation in the lifetime components for energies greater than 8 keV in the thin film $SrTiO_3$ sample clearly show the onset of annihilation events from the film interface and the substrate [Figs. 2(a) and 2(b)]. A low intensity third lifetime component due to large open-volume defects is detected and a short reduced bulk lifetime is resolved, the dominant second lifetime reduces from ~400 to ~270 ps between 8 and 12 keV. For the implantation energies 13–18 keV the average values for the second and third lifetimes are 235(13) ps and 480(70) ps, respectively, these are comparable to the results from near-surface region of the as-received substrate [Figs. 2(e)–2(h)]. However, the intensity of the dominant defect lifetime is higher consistent with near-surface defect formation in the substrate during deposition.

Figure 1 also shows the Doppler broadening spectroscopy detected *S* parameter (defined using $|p_L|<3.1\times10^{-3}m_0c$) depth profiles for the $SrTiO_3$ thin film and single-crystal $SrTiO_3$ samples obtained immediately after the VE-PALS measurements. The increase in the *S* between the substrate value and the plateau in the thin film (5–10 keV) is ~3.9%, it has been suggested that this is consistent with trapping to Sr vacancies or V_{Sr}-nV_O complexes.[25] The further marked increase in *S* toward the surface of film, and the substrate, is often characteristic of the presence of larger open-volume defects. Comparison of Figs. 1(b) and 1(d) with behavior of the positron lifetime components shown in Fig. 2 provide direct evidence for validity of these assumptions.

IV. CONCLUSIONS

In summary that we have shown that the high statistics positron lifetime measurements, made possible by the use of a high intensity positron beam, allow identification of vacancy defects in thin film perovskite oxides and have the capability of achieving subparts per million sensitivities. The depth dependence of the positron lifetime components, shown in Fig. 2, readily identify a near-surface region of depth ~50 nm, where a nanosecond component due to large vacancy clusters is detected, below this layer the bulk of the

film exhibits a uniform distribution of Sr vacancies. A second lifetime component is also present in this region and is attributed to vacancy cluster defects larger than cation divacancy nearest-neighbor oxygen vacancy complexes with the aid of DFT calculations. Insight is also obtained on the interface region and on changes to the top layer of the substrate.

ACKNOWLEDGMENTS

R.A.M. acknowledges the support from the Carnegie Trust for the Universities of Scotland. D.J.K. and R.A.M. acknowledge support of the European Commission Programme under Contract No. RII3-CT-2003-505925.

*d.j.keeble@dundee.ac.uk

[1] J. F. Scott, Science **315**, 954 (2007).
[2] C. H. Ahn, K. M. Rabe, and J. M. Triscone, Science **303**, 488 (2004).
[3] C. H. Ahn, J. M. Triscone, and J. Mannhart, Nature (London) **424**, 1015 (2003).
[4] A. Ohtomo and H. Y. Hwang, Nature (London) **427**, 423 (2004).
[5] E. Bousquet, M. Dawber, N. Stucki, C. Lichtensteiger, P. Hermet, S. Gariglio, J. M. Triscone, and P. Ghosez, Nature (London) **452**, 732 (2008).
[6] R. Ramesh and N. A. Spaldin, Nature Mater. **6**, 21 (2007).
[7] S. Poykko and D. J. Chadi, Phys. Rev. Lett. **83**, 1231 (1999).
[8] D. M. Smyth, *The Defect Chemistry of Metal Oxides* (Oxford University Press, New York, 2000).
[9] R. Merkle and J. Maier, Angew. Chem., Int. Ed. **47**, 3874 (2008).
[10] R. R. Garipov, J. M. Spaeth, and D. J. Keeble, Phys. Rev. Lett. **101**, 247604 (2008).
[11] S. Lenjer, O. F. Schirmer, H. Hesse, and Th. W. Kool, Phys. Rev. B **70**, 157102 (2004).
[12] C. L. Jia and K. Urban, Science **303**, 2001 (2004).
[13] D. A. Muller, N. Nakagawa, A. Ohtomo, J. L. Grazul, and H. Y. Hwang, Nature (London) **430**, 657 (2004).
[14] T. Mizoguchi, Y. Sato, J. P. Buban, K. Matsunaga, T. Yamamoto, and Y. Ikuhara, Appl. Phys. Lett. **87**, 241920 (2005).
[15] R. Krause-Rehberg and H. S. Leipner, *Positron Annihilation in Semiconductors* (Springer-Verlag, Berlin, 1999).
[16] V. J. Ghosh, B. Nielsen, and T. Friessnegg, Phys. Rev. B **61**, 207 (2000).
[17] A. S. Hamid, A. Uedono, T. Chikyow, K. Uwe, K. Mochizuki, and S. Kawaminami, Phys. Status Solidi A **203**, 300 (2006).
[18] D. J. Keeble, S. Singh, R. A. Mackie, M. Morozov, S. McGuire, and D. Damjanovic, Phys. Rev. B **76**, 144109 (2007).
[19] R. A. Mackie, S. Singh, J. Laverock, S. B. Dugdale, and D. J. Keeble, Phys. Rev. B **79**, 014102 (2009).
[20] D. J. Keeble, A. Krishnan, T. Friessnegg, B. Nielsen, S. Madhukar, S. Aggarwal, R. Ramesh, and E. H. Poindexter, Appl. Phys. Lett. **73**, 508 (1998).
[21] D. J. Keeble, B. Nielsen, A. Krishnan, K. G. Lynn, S. Madhukar, R. Ramesh, and C. F. Young, Appl. Phys. Lett. **73**, 318 (1998).
[22] T. Friessnegg, S. Aggarwal, R. Ramesh, B. Nielsen, E. H. Poindexter, and D. J. Keeble, Appl. Phys. Lett. **77**, 127 (2000).
[23] A. Uedono, K. Shimayama, M. Kiyohara, Z. Q. Chen, and K. Yamabe, J. Appl. Phys. **92**, 2697 (2002).
[24] A. Uedono, K. Shimoyama, M. Kiyohara, Z. Q. Chen, K. Yamabe, T. Ohdaira, R. Suzuki, and T. Mikado, J. Appl. Phys. **91**, 5307 (2002).
[25] S. McGuire, D. J. Keeble, R. E. Mason, P. G. Coleman, Y. Koutsonas, and T. J. Jackson, J. Appl. Phys. **100**, 044109 (2006).
[26] T. Friessnegg, S. Aggarwal, B. Nielsen, R. Ramesh, D. J. Keeble, and E. H. Poindexter, IEEE Trans. Ultrason. Ferroelectr. Freq. Control **47**, 916 (2000).
[27] Y. Y. Tse, Y. Koutsonas, T. J. Jackson, G. Passerieux, and I. P. Jones, Thin Solid Films **515**, 1788 (2006).
[28] C. Hugenschmidt, B. Lowe, J. Mayer, C. Piochacz, P. Pikart, R. Repper, M. Stadlbauer, and K. Schreckenbach, Nuc. Instrum. Methods Phys. Res. A **593**, 616 (2008).
[29] P. Sperr, W. Egger, G. Kogel, G. Dollinger, C. Hugenschmidt, R. Repper, and C. Piochacz, Appl. Surf. Sci. **255**, 35 (2008).
[30] M. Stadlbauer, C. Hugenschmidt, and K. Schreckenbach, Appl. Surf. Sci. **255**, 136 (2008).